Article type: Research Paper

Ultrathin, ultra-conformable and free-standing tattoo-able organic light-emitting diodes

Jonathan Barsotti[1,2]*, Alexandros G. Rapidis[3], Ikue Hirata[1], Francesco Greco[1,4], Franco Cacialli[3]*†, Virgilio Mattoli[1]*†

[1] Center for Micro-BioRobotics, Istituto Italiano di Tecnologia
Via R. Piaggio, 34, 56025 Pontedera, PI, Italy

[2] The Biorobotics Institute, Scuola Superiore Sant'Anna
Via R. Piaggio, 34, 56025 Pontedera, PI, Italy

[3] Department of Physics and Astronomy and London Centre for Nanotechnology, University College London, WC1E 6BT, London, UK

[4] Institute of Solid State Physics, NAWI Graz, Graz University of Technology, Petersgasse 16, 8010 Graz, Austria

* Corresponding authors: barsotti.sciresearch@gmail.com; f.cacialli@ucl.ac.uk; virgilio.mattoli@iit.it
† These authors share senior authorship

Keywords: soft electronics, tattoo electronics, ultrathin OLED, free-standing, conformable electronics

Abstract: We demonstrate a novel tattoo-able, ultrathin, green-emitting organic light-emitting diode (OLED) fabricated on top of commercial temporary tattoo paper. The transfer mechanism relies on dissolution of the sacrificial layer typically incorporated in paper-tattoos. The ready-to-use device can be stored on the tattoo substrate and released on the target surface at a later time, simply by a slight wetting of the tattoo paper with water. This approach provides a quick and easy method of transferring OLEDs on virtually any surface. This is particularly appealing, in perspective, for on-skin and disposable electronic applications. Our proof of concept demonstrates, for the very first time, the feasibility of ultrathin operational OLED tattoos. While the performance of such devices is not yet comparable with that of OLEDs on rigid or flexible non-tattoo-able substrates, our results show the potential for an OLED tattoo technology in integrated conformable electronic circuits.

1. Introduction

Flexible electronics is enabling ubiquitous, unperceivable and conformable devices that are highly appealing for applications such as on-skin (or "skin-wearable")[1] unobtrusive sensors for monitoring a variety of parameters relevant to a wide range of applications. These include for example biomedical,[2–4] sport activity and environment monitoring systems.[4,5] Displays are fundamental components, among others, for devices requiring a user interface. Organic light-emitting diodes (OLEDs) are already largely used in the fabrication of flat panel displays for smartphones, TVs, computer monitors, personal digital assistants (PDAs) and other portable devices.[6] In addition, OLEDs are compatible with scalable large-area fabrication techniques such as, but not limited to, ink-jet printing,[7,8] roll-to-roll[9] and screen printing, strongly reducing fabrication costs.[10] Within this context, improving fabrication technologies[11] and materials[8] in order to provide flexible and conformable electronic devices would enable new applications in those scenarios where device stiffness is currently a limitation.[12,13] The reduction of OLED thickness[14] is usually the most obvious strategy to increase device

flexibility and conformability. In addition, OLEDs can offer connectivity via visible light communication (VLC)[15,16] and thus enable implementation of the internet-of-thing (IoT). At present, there is a lack of displays/communication devices offering the properties necessary to enable ultra-flexible[17] and ultra-conformable devices,[18] whereas the development of a versatile ultrathin and ultra-conformable OLED would boost a variety of novel potential applications. It is likely that ultrathin OLEDs integration within electronic skin,[19–21] wearable devices[22] for healthcare and personal monitoring[23] will enable breakthrough applications for novel human interfaces as well as for bio-sensing.

The use of temporary tattoo (TT) substrates provides a promising alternative when considering solutions for ultrathin, conformable and low-cost disposable transferable electronics. This strategy has been adopted for various tattoo-like devices.[24] All of these "Tattoo Electronics" (TE) applications make use of a commercial temporary "tattoo-paper" substrate which enables an easy water-assisted transfer directly onto skin and other surfaces, and provides stable and conformal adhesion to the target surfaces. Zucca *et al*. developed conformable electromyography (EMG) electrodes by deposition of ultrathin conductive poly(3,4-ethylendioxythiophene): poly(styrenesulfonate) (PEDOT:PSS) onto TT with an overall thickness ≈500 nm.[4] Further improvements led to multi-electrode temporary tattoo electrodes which were successfully tested in EMG as well as in electrocardiography (ECG)[5] and electroencephalography (EEG)[25] providing for the first time an easy to use, dry, unperceivable skin contact electrode which also proved to be resilient to perforation by growing hairs. Wang *et al*. proposed a low-cost, 1.5-µm-thick, multifunctional tattoo electrode for simultaneous measurement of skin temperature, skin hydration, electrocardiogram (ECG), and heart rate during perspiration.[26] These applications showed some of the TE advantages for skin-worn healthcare monitoring applications. Applications on surfaces other than human skin were also proposed, and included, for example, a printed TT electrode for organic photovoltaic (OPV).[27] In this case, the electrode was directly transferred onto the solar cell and specifically tailored

for low-light conditions, thereby affording the remarkable photo-conversion efficiency of 7.0% under low illumination conditions. This is only an illustrative example of the promise of the tattoo approach in the development of the fabrication process of OPVs. In addition, owing to the particular nature of the TT constituents, TE also found application in edible electronics.[28] Bonacchini *et al.*, for example, proposed an edible organic field-effect transistor (OFET) on untreated commercial TT paper releasing a transferrable substrate of ethylcellulose. The device operation was demonstrated after transferring on edible substrates with a complex non-planar geometry. Recently a tattoo approach has been presented for obtaining a transferable printed organic photodiode (OPD). Tattoo-able devices reported in the literature exhibited encouraging results in terms of chemical and structural features, compatibility of the paper substrate with electronics fabrication techniques and devices performance, thereby highlighting the potential of TE for low-cost, unperceivable and disposable devices. Despite no true tattoo-like OLED display has been proposed yet, various groups have attempted the development of transferrable OLED. Choi et al., recently proposed a transferrable quantum dot OLED (QLED) with a total thickness of ≈2.6 μm and over 1% external quantum efficiency (EQE).[29] The QLED have remarkable J-V, luminance and EQE characteristics. Furthermore, red-green-blue QLED layers can be combined to enable fabrication of multicolour displays. The QLED transfer mechanism proposed by Choi *et al.* was an intaglio transfer printing. This fabrication technique requires a specific intaglio mould, one for each QLED coloured layer and pattern. Despite showing excellent performance, the QLED transfer process is more complicated than the water-based tattoo transfer one.[4,5,27,28] Developing a truly tattoo-like OLED would provide a quick and easy method of transferring an OLED structure on virtually any surface, and enable a variety of new applications. In this work, we propose a novel, non-encapsulated, green-emitting OLED tattoo device fabricated on top of a commercial TT paper substrate. The device fabrication relies on a combination of ink-jet printing, spin coating and thermal evaporation to deposit the different device layers. This work intends to serve as a proof of concept for the feasibility of tattoo-able,

conformable and disposable OLEDs using commercial tattoo paper as a temporary substrate, with scope for application of the transfer method to arbitrary surfaces.

2. Results and Discussions

2.1. OLED Tattoo structure

We report the OLED tattoo fabrication process in **Figure 1 (a-b)** and the device structure in Figure 1 (c) and (d). The OLED tattoo consists of five layers: the TT paper substrate, the poly(methyl methacrylate) PMMA layer, the PEDOT:PSS bottom electrode, the poly(9,9'-dioctylfluorene-*alt*-benzothiadiazole) (F8BT) green-emitting copolymer active layer and the Al top electrode. We adopted an inverted OLED architecture (Figure 1 (d)), so as to ensure light is emitted "outside", i.e. towards the direction pointing away from the surface on which the device is transferred. In this architecture the highly reflective Al electrode will come in contact with the target object once the OLED is transferred, while exposing the PEDOT:PSS semi-transparent electrode, thereby allowing for light emission. A direct configuration can also be adopted (i.e. with emission into the skin/surface) for applications requiring it, such as photodynamic therapy[30] or pulse-oximetry.[31,32]

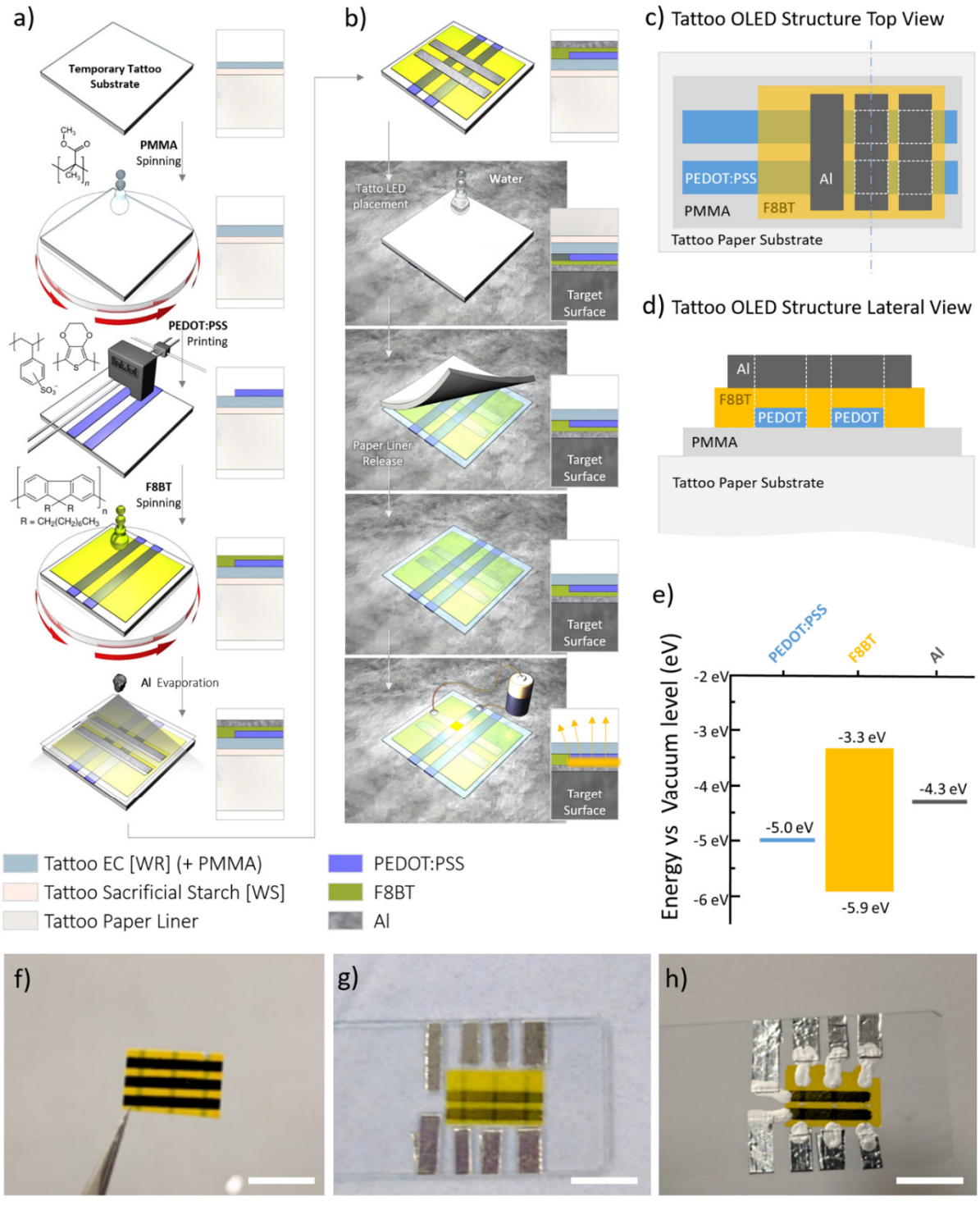

Figure 1: Schematics of the OLED tattoo device: (a) fabrication process and (b) transfer process. Device structure schematics showing (c) top and (d) lateral view. (e) Nominal energy levels referred to the vacuum level for the OLED device structure. Pictures of the OLED tattoo device (f) before and (g) after the transfer on a glass slide and (h) after transfer with electrical contacts for the device characterization. All scale bars are 1 cm.

Use of the TT substrates allows easy handling of the ultrathin device during the whole fabrication and until its final transfer and use. For the sake of brevity, we will refer to it a single layer, but it must be pointed out that it is actually a multi-layered sheet. Specifically, this incorporates three layers (Figure 1a): a water resistant (WR) ethylcellulose (EC) layer on one side and a water soluble (WS) starch/dextrin layer placed between a glassine paper sheet and the WR layer. The layered structure is at the base of the tattoo transfer principle. When the tattoo sheet is moistened from the paper side, water molecules penetrate the paper layer, and are thus able to reach and dissolve the WS intermediate layer (see Figure 1 (b)). The paper layer can then be removed by sliding it away, with the dissolved WS layer acting as a cushion. The WR layer remains attached to the target surface thanks to Van der Waals adhesion forces.[26,33] The WR layer is compatible with ink-jet printing and other deposition techniques.[4,5,27,28] A more detailed description of the TT paper structure and of the main characteristics of the WR layer can be found in the review by Ferrari et al.[24]

In our case, to fabricate the OLED on the tattoo paper, we deposited a first insulating layer of PMMA by spin-coating. The layer had a nominal thickness of about 1.5 μm and a roughness < 2 nm (root mean square, RMS, as determined from AFM surface morphology analysis). The purpose of this layer was to act as a barrier against toluene which otherwise damages the WS layer, eventually preventing a correct tattoo release. The OLED tattoo structure consists of three layers stacked on top of the PMMA: the bottom transparent electrode, the electroluminescent (EL) polymer and the top reflective electrode. We kept the structure minimal, focusing the work on demonstrating the non-encapsulated OLED tattoo feasibility.

The PEDOT:PSS bottom electrodes was deposited by inkjet printing according to the pattern design reported in Figure 1 (c) (surface resistance = 170 ± 30 Ω/sq). This electrode serves both as the semi-transparent electrode and hole-injection layer. On top of the bottom electrode, the electroluminescent F8BT active layer was deposited by spin-coating. Finally, an Al cathode top electrode was deposited by thermal evaporation on top of the structure.

We report the nominal energy levels associated to our OLED tattoo structure in Figure 1 (e). The specific formulation of the PEDOT:PSS electrode that acts as a hole-injection layer, has been reported to have a typical average work function φ_p in the range 5.0-5.2 eV,[34] giving rise to a nominal holes energy barrier in the range ≈ 0.7- 0.9 eV. The Al electrode acts as n-type injection layer, with an estimated work function φ_a= - 3.7-3.8 eV,[35] having taken into account the residual oxygen in the evaporation chamber under our processing conditions. The two overlapping electrodes determine an active area of ~2 mm^2.

Figure 1 (b) displays the OLED tattoo transfer process. The OLED transfer requires the device to be upside down, with the Al top electrode facing toward the target surface. By keeping the OLED Tattoo in the desired position, the backside of the tattoo can be exposed to water. We note here that by using a tissue-like absorber paper or similar tissue, it is possible to exercise an improved control over the amount of water released on the OLED Tattoo. Once the water-soluble layer is fully dissolved (typically in 20 - 30 s) the paper sheet is removed with a sliding movement and the device adheres and conforms to the target surface. We report a picture of the OLED tattoo before (Figure 1 (f)) and after (Figure 1 (g)) the transfer and a picture that show the contacts used to power the device and measure its electrical properties (Figure 1 (h)).

2.2. Device characterization

We acquired tapping mode atomic force microscopy (AFM) topographic images of the OLED tattoo layers of 1 μm × 1 μm for each device layer (**Figure 2 (a, i-iv)**). These refer to devices transferred on silicon substrate (see Experimental Section for more details). The PMMA functionalization layer surface, with topographic variations of only 3 nm over the whole image range is visible in Figure 2 (a, i) and confirms the relatively smooth nature of the surface.[4,24] The PEDOT:PSS ink-jet printed bottom electrode also reveals a fairly homogeneous surface, as visible in Figure 2 (a, ii). We note that the roughness and thickness homogeneity of the electrodes are important because they directly affect the homogeneity of the ultrathin F8BT

active layer. Defects in the underlying layers, such as PMMA or PEDOT:PSS, could induce critical defects in the F8BT layer and compromise the whole tattoo device operation. The homogeneity of the PEDOT:PSS electrode enabled preparation of an almost defect-free surface of the F8BT layer as shown in Figure 2 (a, iii). Some Al aggregates are visible in the AFM of top electrode, with a thickness up to 120 nm (Figure 2 (a, iv)). The aggregates do not affect the OLED structure integrity because they are forming in the last deposited layer, at the very top of the OLED structure. We did not observe any device adhesion problem on surfaces such as glass, paper, metals, plastic and other organic materials. We attributed the formation of large Al aggregates to the evaporating procedure we used, consisting of a first gentle step at slow deposition rate (0 - 50 nm) and a second fast rate step (50 - 200 nm). The optimization of the second deposition step was beyond the scope of this work. However, the formation of large Al aggregates should nevertheless be avoided or minimized and should be addressed in future development of the OLED tattoo, in order to further improve the device adhesion.

The full stack thickness of the transferred OLED tattoo (on a glass substrate) is shown in Figure 2 (b). The measurement was carried out by stylus profilometry across a scratch in the OLED active area. The average height for both the device and the glass substrate are also reported (dashed red lines). The inset shows the optical image of the scratch where the measurement was acquired. Overall, the total thickness of the device including the released TT substrate is 2.3 ± 0.1 μm.

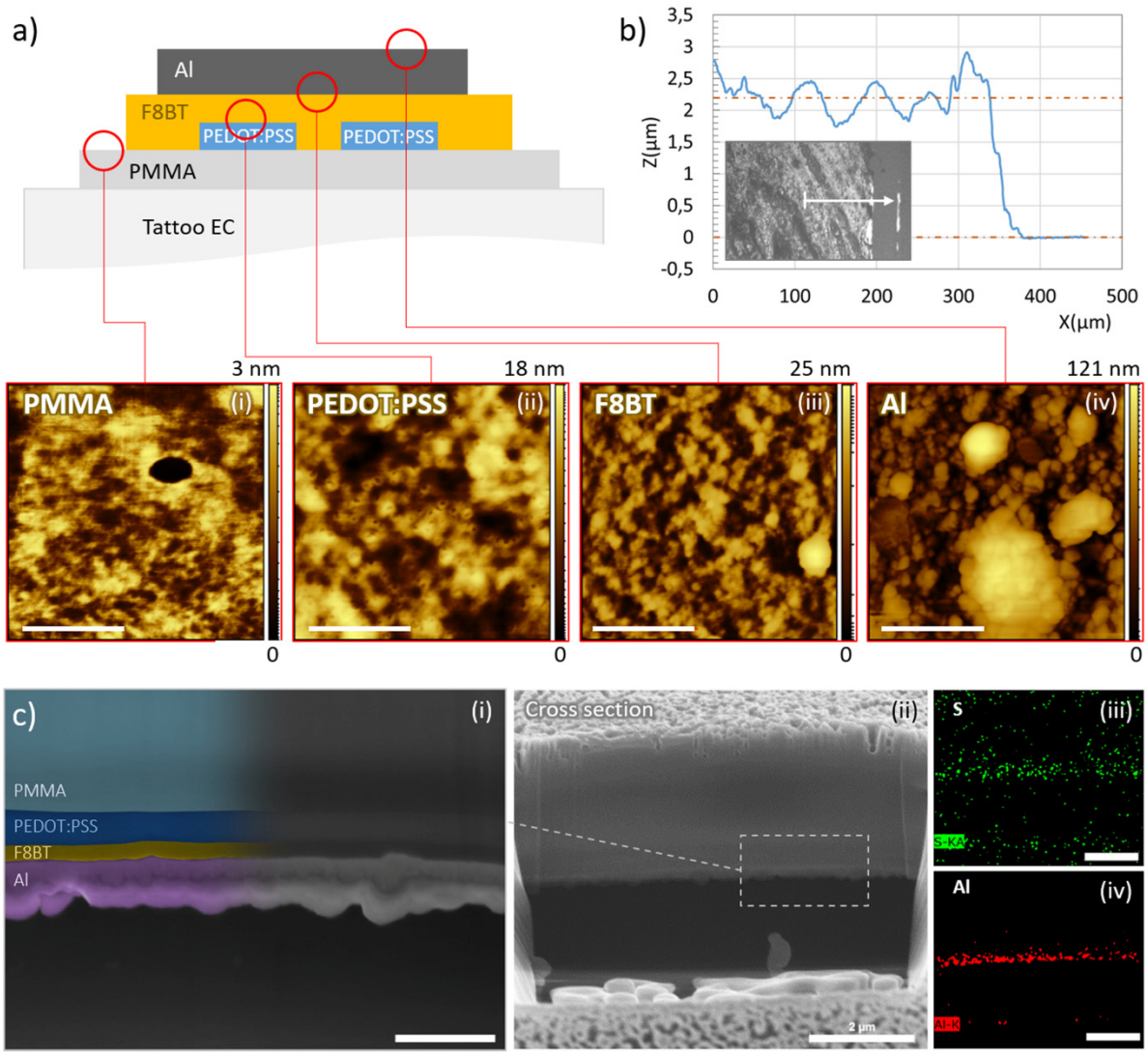

Figure 2: (a) Lateral view of the OLED tattoo schematic showing representative measurement acquisition points: AFM topography of (a, i) PMMA functionalization layer, (a, ii) PEDOT:PSS bottom electrode, (a, iii) F8BT active layer and (a, iv) aluminium top electrode. AFM images (a, i-iv) scale bar, 400 nm. (b) Representative profilometry of the full device tattoo after the release on glass silicon wafer and scratched with a needle in correspondence of the active area (full stack device). (c)SEM image of device cross-section (c, i) zoom, clearly showing the device layers and (c, ii) associated cross-section overview of the point used for the measurement. (c, iii) Elemental EDX analysis collected at the same position of image (c, i), showing the presence of (c, iii) sulphur and (c, iv) Al in correspondence of the organic layers (F8BT and PEDOT:PSS) and the Al top electrode, respectively. SEM images scale bars: (c, i) 500 nm, (c, ii-iv) 2 µm.

The OLED tattoo cross-section, obtained by Focused Ion Beam (FIB) milling, is shown in Figure 2 (c). The three layers are clearly visible in Figure 2 (c, i) with the thin F8BT active layer (thickness = 76 ±6 nm) sandwiched between the PEDOT:PSS electrode (top, thickness = 142 ±7 nm) and the Al electrode (bottom, thickness = 211 ±24 nm). All intermediate layers' thicknesses have been estimated by the cross-section SEM image. Figure 2 (c, ii) shows the cut made by the FIB. Identification of layers is supported by an EDX elemental mapping analysis of aluminium (electrode, Figure 2 (iii)) and sulphur (active layer and transparent electrode, Figure 2 (iv)). Despite only permitting qualitative considerations due to limited spatial resolution, the elemental analysis images allow identification of the different layers of the OLED device. The overall tattoo thickness estimated from SEM images, assuming a thickness of ≈ 1.5 μm and ≈ 0.5 μm respectively for PMMA and EC layers, is 2.5±0.1 μm. Such a value is in line with the measured overall thickness of 2.3 ± 0.1 μm, measured by profilometry.

We report the current density–voltage–light emission (JVL) characteristics of the tattoo OLED devices in **Figure 3 (a)**. Light emission reaches a radiance peak of ~ 5 x 10^{-3} mW/cm^2 at an applied voltage of 14 V and a luminance of ~ 0.05 cd/m^2, with the turn-on voltage at ~ 8 V. The light emission output is enough to verify the device is on with the naked eye. As a comparison, a more optimized structure of typical encapsulated OLEDs with a structure glass/ITO/PEDOT:PSS/F8BT/Ca/Al achieves ~1 mW/cm^2.[36] While there is still room for improvement, given the nature of the tattoo devices, the values achieved are remarkable considering the measurements are carried out in ambient conditions after exposure to water for the transfer process, without any encapsulation. The EQE is in the range 0.0162 - 0.0104 %, which is 1-2 orders of magnitude lower than typical values obtained from optimized devices prepared on glass substrates in inert conditions and encapsulated, thus indicating significant margins for improvement by optimisation of the deposition and encapsulation procedures. Other "tattoo-like" devices, such as the QLEDs reported by Choi et al.,[29] with over 1% EQE,

also showed better performance. We note however, that despite affording remarkable J-V characteristic, luminance and EQE, as well as offering the possibility to combine red-green-blue colours, the QLED transfer mechanism proposed by Choi *et al.* relies on an intaglio transfer printing. Here, we demonstrate a truly tattoo-like device that remain the main advantage of the proof-of-concept device proposed in this work. Furthermore, our device showed a total thickness of 2.3 μm, that we expect to be further reduced below 2 μm with the thickness optimization of both the PMMA layer and of the Al top electrode.

2.3. OLED Tattoo operation on complex-shaped objects

To demonstrate the feasibility of the proposed tattoo approach for a transferable OLED, we transferred OLED tattoos on some common objects (Figure 3, (b) - (f)). Once completely dried (< 5 minutes), the devices can be wired and switched on. In particular, Figure 3 (b) shows the device on a standard flat glass slide used to test the devices under reproducible conditions. Figure 3 (c) show an OLED tattoo transferred on a commercial plastic bottle. The OLED tattooed onto an orange, reported in Figure 3(d), displays conformability on relatively rough natural organic surfaces. Figure 3 (e) shows a 4-pixel OLED tattoo transferred on a paper packaging. The two insets show other two pixels of the same device. Finally, we report an ultra-thin, free-standing OLED in Figure 3 (f). We were also able to use a Poly(Vinyl Formal) (PVF) film as a supporting free-standing nanosheet,[37,38] to fabricate free-standing OLEDs. We could switch on OLEDs on such ultrathin suspended PVF nanosheets (handled thanks to appropriate plastic frames), so as to demonstrate the compatibility of tattoo-able OLEDs with fabrication of free-standing devices. The free-standing OLED has a total thickness of 2.5 μm (PVF nanosheet included), and is thinner than other free-standing OLEDs reported so far.[39] The inset of Figure 3 (f) shows another electroluminescing pixel on the same nanosheet. These examples illustrate how the tattoo-like approach enables an easy way to transfer the OLED tattoo on virtually any surface, thereby also allowing fabrication of membrane OLED.

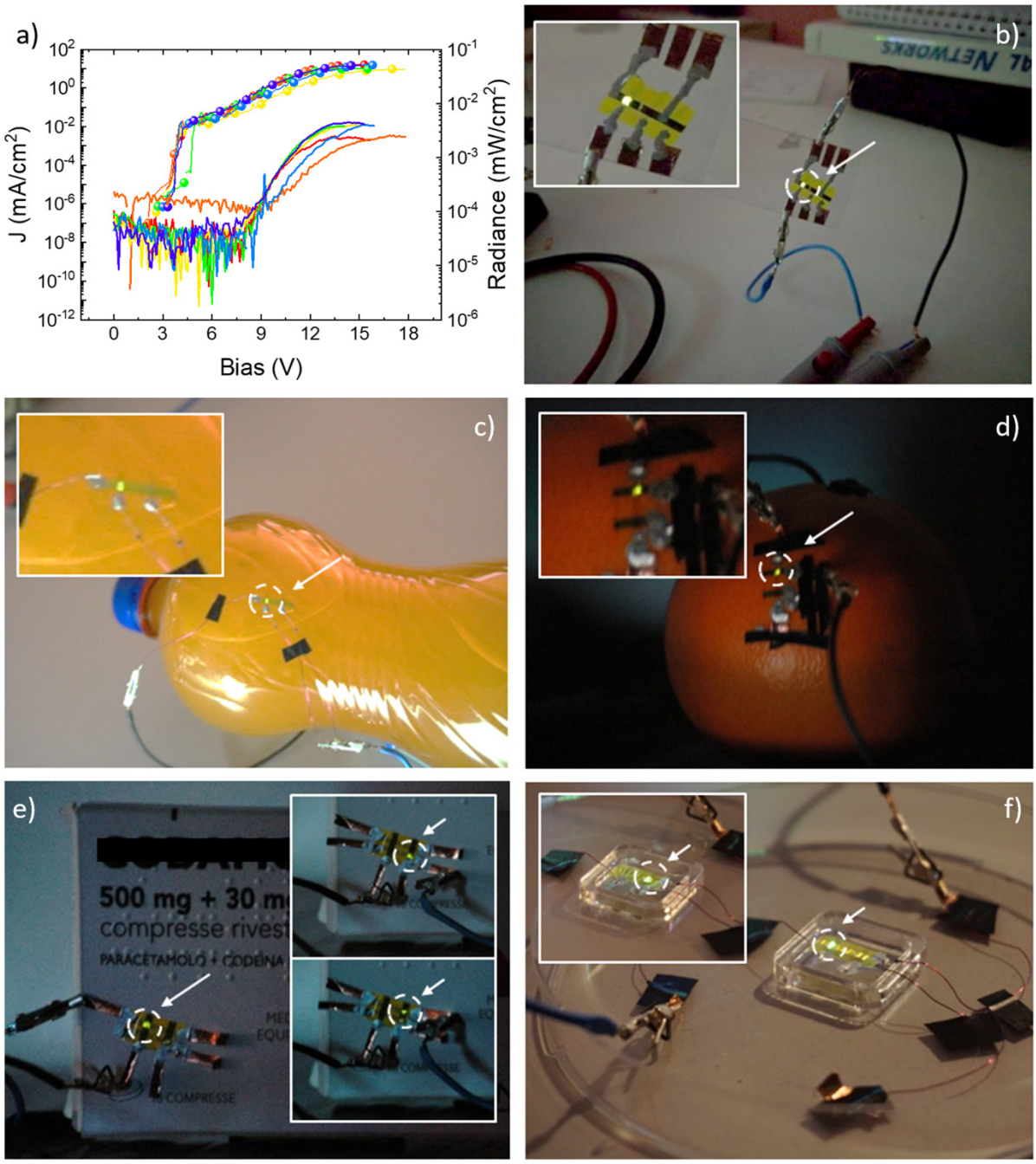

Figure 3: (a) Transferred tattoo OLED current density J (lines with circle markers) and Radiance (lines without markers) vs. applied voltage(Bias). Each different colour refers to various samples (data of 6 samples is shown). (b-f) Pictures showing working OLED tattoo devices transferred on: (b) a glass slide, used for device characterization; (c) a commercial plastic bottles; (d) an orange; (e) a paper packaging. (f) OLED tattoo device transferred on a freestanding PVF nanosheet (t < 140 nm) to demonstrate the feasibility of an ultrathin free-standing OLED with a total thickness ~ 2.5 µm.

We consider there are significant margins for improvement of the performance (e.g. efficiency, lifetime, and operating voltage), expected for example by fabricating the devices under controlled atmosphere (the fabrication was entirely carried out in air in our experiments) and by optimising the encapsulation. These developments will aim to minimise exposure to air and water of the active parts of the devices during the transfer and subsequent operation. Both air and water/moisture are well known to be responsible for damage and degradation of the active material and of the electrodes/related interfaces. Despite the prolonged exposure to stressful agents, the OLED operation was not totally compromised, as demonstrated by the EL data and the optical images of working devices reported in this work (Figure 3). Future work will have to address the extension of device lifetime and air-stability, as well as the emissive area homogeneity (partially also compromised by air-exposure).

The non-uniform emission area is also due to gradual and randomly distributed degradation generated in the F8BT by the absence of encapsulation. It is well known that OLEDs devices benefit substantially from encapsulation barriers compared to other devices, such as thin-film batteries, radio frequency identification (RFID) devices or food packaging, to name but a few examples. The OLEDs estimated water vapour transmission rate (WVTR) is 1×10^{-6} $g \cdot m^{-2} \cdot day^{-1}$ and the oxygen transmission rate (OTR) is 1×10^{-5}-10^{-3} $cm^3 \cdot m^{-2} \cdot day^{-1}$.[10] Al electrode and PMMA functionalization layers barrier properties are not enough to satisfy oxygen and water permeation rates required to ensure OLEDs longevity. While the OLED tattoo presented here can only operate for a few minutes in air and without encapsulation, we note that its intended purpose is to provide an ultra-cheap and disposable tattoo-like OLED, to be possibly integrated in skin-worn or wearable devices for healthcare and personal monitoring. With this in mind, we also remark that some of the strict requirements about barrier properties and maximum WVTR and OTR could possibly be relaxed in some envisioned applications, for which an operative lifetime of 1 day or even few hours is already sufficient to satisfy the typical average duration of a medical examination or a sport challenge, that rarely lasts over 3 hours.

In order to further extend operative lifetime of OLED devices, the improvement of encapsulation strategy is the most direct way to follow, but other approaches could be considered.[40] In particular, adoption of materials intrinsically more robust with respect to oxidation and water/oxygen initiated chemistry might also be possible. This is a significant challenge given the inherent anti-bonding nature of the excited states of conjugated semiconductors, which makes them prone to such side-reactions, but we note that the lifetime of OLEDs on rigid substrates has also been increased significantly since the first studies,[41] and that similar progress could reasonably be expected here. For example, it should be possible to capitalise on lessons learned in the development of bioelectronics durable implants based on organic materials,[42] also considering hybrid organic/inorganic encapsulation layers,[43] or looking to new appealing novelty, such as air stable radical polymers, recently employed for the fabrication off several organic electronic devices.[44]

From application side, strategies to integrate tattoo OLED technology with other electronic devices on unconventional substrates could be also further investigate. For example, recently conductive carbon inks have been successfully employed by Wang *et al.* to fabricate deformable electrical connections to integrate different components onto unconventional substrates for electronics, such as paper.[45] Following a similar approach, the tattoo OLED could be integrated with other electronic components, such as batteries or capacitors to provide the necessary power, for example, and more generally enable the realization of plug and play devices.

Despite the current limitations, and in view of the considerations above, we consider therefore this work to be of remarkable importance as the first demonstration of disposable OLED tattoos with scalable and ultra-cheap fabrication techniques. Optimisation of the device structure with additional functional layers, adoption of inherently more stable materials, and/or of appropriate encapsulation will improve performance and extend OLED tattoos lifetime.[46] We expect that the uniformity of the emissive area will also benefit from such structural improvements.

3. Conclusion

In this work, we reported a novel tattoo-able, ultrathin OLED device. The device can be fabricated on top of a commercial temporary tattoo paper, in air and without any encapsulation. The OLED tattoo transfer mechanism relies on an actual tattoo-like transfer, in which the ready-to-use device can be stored on the tattoo substrate and released on the target surface at a later time, by simply using a small amount of water. Although clearly exposed to non-ideal environmental conditions during the fabrication and the transfer steps, we demonstrated successful operation of such OLED tattoos for the very first time. While stability, J-V characteristics, radiance and EQE need further improvement for applications, our results show the potential for implementing an OLED tattoo technology in integrated conformable electronic circuits, potentially also paving the way for a new generation of portable, low cost and low power displays.

4. Experimental Section/Methods

Tattoo paper foils (The Magic Touch Ltd., UK) were cut in rectangular pieces of approximately 2.2 cm x 3.0 cm. Each piece of tattoo paper was fixed to a glass substrate (VWR® Plain Micro Slides, 75 mm x 25 mm x 1 mm, VWR International) using Kapton tape (Tesa s.p.a.) along all the four tattoo edges in order to spread the paper out on the glass support, obtaining a fixed flat surface suitable for spin coating deposition techniques. The Kapton chemical resistance also avoided lateral solvents penetration into the tattoo paper during device fabrication. In order to prevent toluene penetration under the WR layer during the fabrication, the WR layer of TT was coated with a PMMA layer. This provided an efficient solution against solvent penetration, also improving tattoo surface wettability. The functional PMMA (average Mw = 120 kDa, Sigma Aldrich) layer was obtained by spin coating 170 µl of 80 mg/ml PMMA solution in n-butyl acetate (for analysis, purity > 99 %, Carlo Erba Reagents) at a speed of 3000 rpm for 60 s. A soft bake step was carried out at 60°C for 10 minutes in order to remove solvent residuals. Bottom electrodes were fabricated by ink-jet printing of PEDOT:PSS with a Dimatix Materials Printer (DMP-2800, Fujifilm Corp., Japan). PEDOT:PSS ink (Clevios P Jet 700, Heraeus, Germany) was filtered (hydrophilic, Minisart, average pore size 0.2 µm, Sartorius) and then ink-jet printed in a set of parallel lines of width 1 mm pattern (drop spacing 20 dpi, plate temperature 40°C, head at room temperature). The overlap of each bottom electrode line with a successively fabricated top electrode line (2 mm wide) defined the final OLED active area. The ink-jet printer plate temperature was kept at a temperature of 40°C for the whole printing session in order to allow faster water evaporation obtaining more homogeneous PEDOT:PSS surfaces and clear pattern edges. Once printed, PEDOT:PSS bottom electrodes were annealed at 120 °C for 20 minutes on hot plate. The polymeric active layer was deposited on the ink-jet patterned PEDOT:PSS electrodes, by spin coating a 10 mg/ml F8BT (Poly(9,9-dioctylfluorene-alt-benzothiadiazole), Mw = 15 000 - 200 000 kDa, American Dye Source Inc.) solution in Toluene (puriss p.a., purity > 99.7 %, Sigma Aldrich) at a speed of 1200 rpm for 90 s, on the

PMMA/TT substrate. The spun F8BT was left drying under ambient condition overnight. The mask pattern used for evaporated aluminium electrodes was made of parallel lines of 2 mm of width cut out from a 1.2 mm thick poly(tetraflouroethylene) (PTFE) sheet (supplied by RS Components S.r.l.), using a laser cutter (Versa Laser VLS3.50, Universal Laser Systems Inc.). The sample was fixed to the evaporator mask ensuring that the ink-jet patterned PEDOT:PSS bottom electrode lines were orthogonal to the mask pattern lines, determining a rectangular overlapping area. The ≈ 200 nm top Al electrode on the active layer was evaporated in a two-steps deposition: during the first step we deposited a layer of 50 nm at ~0.01-0.06 nm/s. During the second step we deposited a second Al layer to reach the final thickness of about 200 nm. Thermal evaporation was carried out using an Edwards A306 Box Evaporator (1.8x10-6 - 7x10-7 mbar) and Al source material purchased from Sigma Aldrich. OLED full stack thickness characterization was performed by means of a P-6 stylus profilometer (KLA Tencor, USA) averaging over 9 estimated values randomly acquired on the tattoo after the release on silicon wafer and scratched with a needle in correspondence of the active area (full stack device). Cross-sectional SEM image of a tattoo OLED transferred on a silicon substrate have been created and characterised by using a Dual Beam FIB/SEM Helios Nano-Lab 600i (FEI) with following operative parameters: 30kV kV accelerating voltage and 80pA current for ion beam milling, and 10 kV accelerating voltage and variable magnification for e-beam imaging. For eliminating charging effect for imaging, the sample was preliminary prepared by Au deposition (layer about 40nm) using AC sputtering. Elemental mapping analysis of aluminium and sulphur has been performed by using the integrated EDX module. The thickness of intermediated layers of PEDOT:PSS, F8BT and Al was evaluated by two different cross-sectional SEM images, averaging the measure of 5 points for each layer for each image. Topography AFM surface images (1 μm × 1 μm) of the OLED devices picked-up on silicon substrates were acquired in Tapping Mode operation (amplitude set-point = 2.1 V, resonant frequency = 126 kHz) by means of an Innova AFM (Veeco, at present Bruker; tip: NSG01 Non-Contact Silicon Probes produces

by NT-MDT Spectrum Instruments, fR = 150 kHz, k = 5.1 N/m). AFM samples preparation: we placed the tattoo above a bowl of water with the device facing upward, leaving the WS layer to dissolve. The paper automatically separates from the WR layer falling to the bottom of the bowl, leaving the tattoo WR layer with the OLED device on top of it, floating on the water surface. We then picked-up the tattoo using a glass slide. We dried it under environmental conditions before measuring the profile. This procedure permitted us to maintain the same stack layer order of the device before its release for the surface and profile characterization. The use of a rigid substrate, such as glass slides, prevents artefacts induced by the tattoo glassine paper bending without altering the tattoo roughness (cover slip RMS roughness < 1 nm[47]).

Electrical measurements were carried out by means of a Keithley 2400 source metre (used for both current measurement and voltage supply). The OLEDs tattoo optical output was measured with a calibrated silicon photodiode and the EL spectra were collected using an Andor Shamrock 163 spectrograph coupled with an Andor Newton EMCCD. The whole electrical characterization of all the OLEDs tattoo devices reported in this work were performed on transferred devices on flat glass substrates.

Acknowledgements

This work was supported by the EU H2020 ETN SYNCHRONICS under grant agreement 643238. FC acknowledges the receipt of a Royal Society Wolfson Research Merit Award. We also thank the EPSRC for support via grant EP/P006280/1.

References

[1] A. J. Bandodkar, W. Jia, J. Wang, *Electroanalysis* **2015**, *27*, 562.

[2] R. Shinar, J. Shinar, *Organic Electronics in Sensors and Biotechnology*, McGraw-Hill, **2009**.

[3] S. Lai, F. A. Viola, P. Cosseddu, A. Bonfiglio, *Sensors* **2018**, *18*, 688.

[4] A. Zucca, C. Cipriani, Sudha, S. Tarantino, D. Ricci, V. Mattoli, F. Greco, *Adv. Healthc. Mater.* **2015**, *4*, 983.

[5] L. M. Ferrari, S. Sudha, S. Tarantino, R. Esposti, F. Bolzoni, P. Cavallari, C. Cipriani, V. Mattoli, F. Greco, *Adv. Sci.* **2018**, 1700771.

[6] L. Zhigang, M. Hong, *Organic light-emitting materials and devices* (Eds.: Li, Z.; Meng, H.), CRC Press, **2007**.

[7] M. Mizukami, S.-I. Cho, K. Watanabe, M. Abiko, Y. Suzuri, S. Tokito, J. Kido, *IEEE Electron Device Lett.* **2017**, *39*, 1.

[8] D. Li, W.-Y. Lai, Y.-Z. Zhang, W. Huang, *Adv. Mater.* **2018**, *1704738*, 1704738.

[9] T. Furukawa, M. Koden, *IEICE Trans. Electron.* **2017**, *E100-C*, 949.

[10] M. Caironi, Y.-Y. Noh, *Large Area and Flexible Electronics* (Eds.: Caironi, M.; Noh, Y.-Y.), Wiley-VCH, **2015**.

[11] S. Nagels, W. Deferme, *Materials (Basel).* **2018**, *11*, 375.

[12] J. Song, H. Lee, E. G. Jeong, K. C. Choi, S. Yoo, *Adv. Mater.* **2020**, *1907539*, 1907539.

[13] L. M. Ferrari, S. Taccola, J. Barsotti, V. Mattoli, F. Greco, In *Organic Flexible Electronics*, Elsevier, **2021**, pp. 437–478.

[14] M. S. White, M. Kaltenbrunner, E. D. Głowacki, K. Gutnichenko, G. Kettlgruber, I. Graz, S. Aazou, C. Ulbricht, D. A. M. Egbe, M. C. Miron, Z. Major, M. C. Scharber, T. Sekitani, T. Someya, S. Bauer, N. S. Sariciftci, *Nat. Photonics* **2013**, *7*, 811.

[15] P. A. Haigh, F. Bausi, Z. Ghassemlooy, I. Papakonstantinou, H. Le Minh, C. Fléchon, F. Cacialli, *Opt. Express* **2014**, *22*, 2830.

[16] A. Minotto, P. A. Haigh, Ł. G. Łukasiewicz, E. Lunedei, D. T. Gryko, I. Darwazeh, F. Cacialli, *Light Sci. Appl.* **2020**, *9*, 70.

[17] D. J. Lipomi, Z. Bao, *MRS Bull.* **2017**, *42*, 93.

[18] X. Huang, Y. Qu, D. Fan, J. Kim, S. R. Forrest, *Org. Electron.* **2019**, *69*, 297.

[19] S. Bauer, *Nat. Mater.* **2013**, *12*, 871.

[20] M. L. Hammock, A. Chortos, B. C. K. Tee, J. B. H. Tok, Z. Bao, *Adv. Mater.* **2013**, *25*, 5997.

[21] T. Yokota, P. Zalar, M. Kaltenbrunner, H. Jinno, N. Matsuhisa, H. Kitanosako, Y. Tachibana, W. Yukita, M. Koizumi, T. Someya, *Sci. Adv.* **2016**, *2*, e1501856.

[22] D. Yin, J. Feng, N.-R. Jiang, R. Ma, Y.-F. Liu, H.-B. Sun, *ACS Appl. Mater. Interfaces* **2016**, *8*, 31166.

[23] Y. Liu, M. Pharr, G. A. Salvatore, *ACS Nano* **2017**, *11*, 9614.

[24] L. M. Ferrari, K. Keller, B. Burtscher, F. Greco, *Multifunct. Mater.* **2020**, *3*, 032003.

[25] L. M. Ferrari, U. Ismailov, J.-M. Badier, F. Greco, E. Ismailova, *npj Flex. Electron.* **2020**, *4*, 4.

[26] Y. Wang, Y. Qiu, S. K. Ameri, H. Jang, Z. Dai, Y. Huang, N. Lu, *npj Flex. Electron.* **2018**, *2*, 6.

[27] N. Piva, F. Greco, M. Garbugli, A. Iacchetti, V. Mattoli, M. Caironi, *Adv. Electron. Mater.* **2017**, *1700325*, 1.

[28] G. E. Bonacchini, C. Bossio, F. Greco, V. Mattoli, Y.-H. Kim, G. Lanzani, M. Caironi, *Adv. Mater.* **2018**, 1706091.

[29] M. K. Choi, J. Yang, K. Kang, D. C. Kim, C. Choi, C. Park, S. J. Kim, S. I. Chae, T. H. Kim, J. H. Kim, T. Hyeon, D. H. Kim, *Nat. Commun.* **2015**, *6*, 1.

[30] I. D. W. Samuel, C. Lian, M. Piksa, K. Matczyszyn, K. Yoshida, S. Persheyev, K.

Pawlik, F. Cabral, M. Ribeiro, J. Lindoso, In *Organic and Hybrid Sensors and Bioelectronics XIII* (Eds.: Shinar, R.; Kymissis, I.; List-Kratochvil, E. J.), SPIE, **2020**, p. 10.

[31] C. M. Lochner, Y. Khan, A. Pierre, A. C. Arias, *Nat. Commun.* **2014**, *5*, 5745.

[32] Y. Khan, A. E. Ostfeld, C. M. Lochner, A. Pierre, A. C. Arias, *Adv. Mater.* **2016**, *28*, 4373.

[33] B. N. Chapman, *J. Vac. Sci. Technol.* **1974**, *11*, 106.

[34] W. Lövenich, *Polym. Sci. Ser. C* **2014**, *56*, 135.

[35] R. I. R. Blyth, S. A. Sardar, F. P. Netzer, M. G. Ramsey, *Appl. Phys. Lett.* **2000**, *77*, 1212.

[36] S. Baysec, A. Minotto, P. Klein, S. Poddi, A. Zampetti, S. Allard, F. Cacialli, U. Scherf, **2018**, *61*, 932.

[37] S. H. Baxamusa, M. Stadermann, C. Aracne-Ruddle, A. J. Nelson, M. Chea, S. Li, K. Youngblood, T. I. Suratwala, *Langmuir* **2014**, *30*, 5126.

[38] J. Barsotti, I. Hirata, F. Pignatelli, M. Caironi, F. Greco, V. Mattoli, *Adv. Electron. Mater.* **2018**, *1800215*, 1.

[39] S. Jun, B.-K. Ju, J.-W. Kim, *Curr. Appl. Phys.* **2017**, *17*, 6.

[40] E. G. Jeong, J. H. Kwon, K. S. Kang, S. Y. Jeong, K. C. Choi, *J. Inf. Disp.* **2020**, *21*, 19.

[41] F. Cacialli, R. H. Friend, S. C. Moratti, A. B. Holmes, *Synth. Met.* **1994**, *67*, 157.

[42] Z. Chen, S. N. Obaid, L. Lu, *Opt. Mater. Express* **2019**, *9*, 3843.

[43] E. Song, J. Li, J. A. Rogers, *APL Mater.* **2019**, *7*, 050902.

[44] L. Ji, J. Shi, J. Wei, T. Yu, W. Huang, *Adv. Mater.* **2020**, *32*, 1908015.

[45] T. Wang, Y. Zhang, Y. Yan, C. G. Jones, D. G. Lidzey, *J. Disp. Technol.* **2016**, *12*, 583.

[46] E. Kim, J. Kwon, C. Kim, T.-S. Kim, K. C. Choi, S. Yoo, *Org. Electron.* **2020**, *82*,

105704.

[47] A. Rasmuson, E. Pazmino, S. Assemi, W. P. Johnson, *Environ. Sci. Technol.* **2017**, *51*, 2151.

Table of Content

We demonstrate a novel tattoo-able, ultrathin, green-emitting organic light-emitting diode (OLED) fabricated on top of commercial temporary tattoo paper. The transfer mechanism relies on dissolution of the sacrificial layer typically incorporated in paper-tattoos. This approach provides a quick and easy method of transferring OLEDs on virtually any surface. This is particularly appealing, in perspective, for on-skin and disposable electronic applications.